

The response of a turbulent boundary layer to a step change in surface roughness. Part 2. Rough-to-smooth

By R. A. ANTONIA AND R. E. LUXTON

Department of Mechanical Engineering, The University of Sydney

(Received 4 December 1971)

An experimental study of the structure of the internal layer which grows downstream from a rough-to-smooth surface change shows it to be essentially different from that studied by Antonia & Luxton (1971*b*) for the case of a smooth-to-rough perturbation. The rate of growth of the internal layer is less than that for the smooth-to-rough step and it appears that the more intense initial rough-wall flow dictates the rate of diffusion of the disturbance for a considerable distance. Inside the internal layer the mixing length l is increased relative to the equilibrium distribution $l = \kappa y$. A turbulent energy budget shows that the advection is comparable with the production or dissipation, whilst there seems to be some diffusion of energy into the internal-layer region close to the wall. The boundary layer, as a whole, recovers much more slowly following a rough-to-smooth change than following a smooth-to-rough change, and at the last measuring station (16 boundary-layer thicknesses from the start of the smooth surface) the distributions of mean velocity and Reynolds shear stress are far from self-preserving.

1. Introduction

There have been few experimental investigations in wind tunnels of the flow field downstream from a rough-to-smooth step change in surface roughness. However, Jacobs (1939) used the measured mean velocity profiles downstream from a rough-to-smooth change in a fully developed channel flow to calculate the shear stress distributions across the flow. These distributions indicate that the wall shear stress attains its new equilibrium value almost immediately, but the shear stress in the outer part of the flow readjusts slowly to the new surface condition. At a distance of approximately 25 channel half-heights downstream from the step, the shear stress profile is significantly different from the fully developed linear distribution. In contrast, a distance of only about 17 channel half-heights is required before a linear shear stress profile is established downstream from a smooth-to-rough step, also studied by Jacobs. Makita's (1968) measurements of the Reynolds shear stress in a channel show, however, that the rate of adjustment of the shear stress downstream from a rough-to-smooth step is not significantly different from that for the smooth-to-rough case. In both cases, a distance of 20 channel half-heights from the step is not sufficient

to establish the fully developed linear shear stress profile. The drag-plate measurements of Bradley (1965) in the atmosphere indicate that, downstream from a rough-to-smooth step, a longer fetch is required (in comparison with the smooth-to-rough step case) before the surface shear stress attains its new equilibrium value. The only available experimental investigation of the rough-to-smooth step in a wind-tunnel boundary layer is that of Taylor (1962), who measured mean velocity profiles only in a weak favourable pressure gradient. For the region near the wall and in the immediate vicinity of the step, these profiles were found, somewhat surprisingly, to fit the universal logarithmic velocity distribution for a smooth-wall equilibrium boundary layer, thus suggesting that the flow near the wall attains an equilibrium state almost immediately downstream from the discontinuity.

This paper describes an experimental study of how a zero-pressure-gradient turbulent boundary layer responds to a sudden change from a rough surface to a smooth surface. One of the aims of this study has been to obtain a set of measurements which could be compared directly with those obtained for the smooth-to-rough change. Such a comparison should clarify some of the discrepancies mentioned above. Also, the mean velocity and turbulence structure near the surface of the rough-wall boundary layer are considerably different from those in a smooth-wall layer (see Antonia & Luxton 1971*a*). The present study, together with the findings of Antonia & Luxton (1971*b*), hereafter referred to as Part 1, should therefore provide a useful opportunity for assessing the effect of the upstream boundary layer on the development of the disturbed flow downstream from the step.

From the present study of the mean flow and turbulence structures of the perturbed region near the smooth wall it is shown that a logarithmic mean velocity distribution has little physical basis in this case. The non-equilibrium nature of the wall region of the internal layer is confirmed by the turbulent energy balance (§ 6), which shows the advection term to be of the same order as the production of turbulent energy. The changes in the turbulence structure of the internal layer (§ 5) are much less pronounced than those which occur immediately downstream from the smooth-to-rough step.

It is also found that the mean velocity and turbulence structure of the outer layer readjust slowly to the perturbation and fail to assume self-preserving distributions at the last measurement station, approximately 16 boundary-layer thicknesses from the change.

2. Experimental arrangement

The experimental facilities used in this investigation were the same as those described in Part 1 except for the configuration of the tunnel floor. The floor consisted of 8 ft of smooth surface followed by 4 ft of 'k-type' rough surface, then a further 4 ft of smooth surface. The smooth surfaces were aligned with the crests of the $\frac{1}{8}$ in. square section roughness elements. These were placed transversely across the floor at a streamwise pitch of $\frac{1}{2}$ in. as in Part 1.

Measurements were made under zero-pressure-gradient conditions at reference

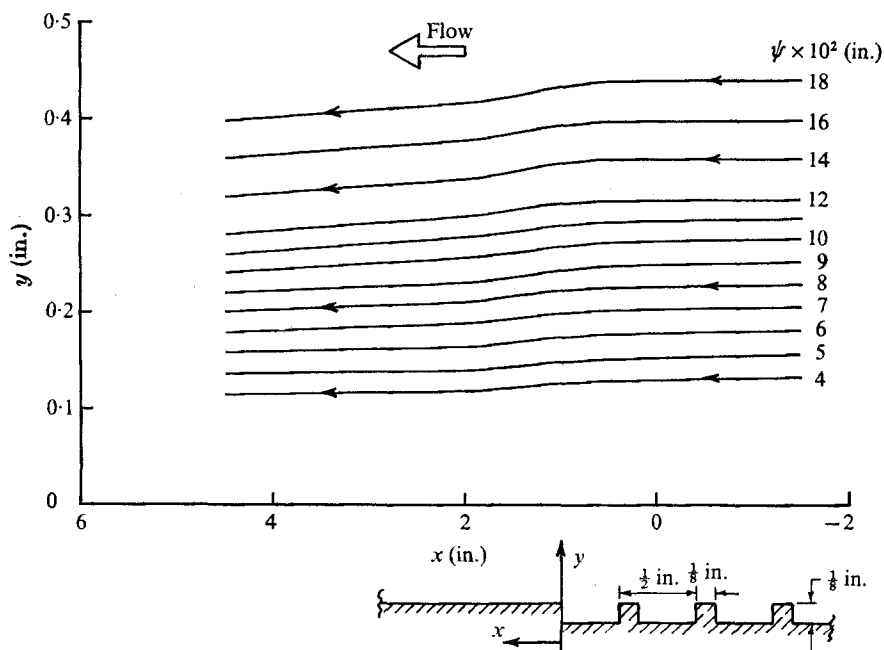


FIGURE 1. Geometry of surface and experimental mean streamlines in vicinity of step ($U_1 \delta_s / \nu \approx 2.6 \times 10^4$). The streamline function ψ is defined as

$$\psi = \int_0^y U/U_1 dy.$$

speeds of 18 and 33 ft/s. The corresponding Reynolds numbers based on the 99.5% boundary-layer thickness δ_s at the end of the 4 ft of rough surface were $U_1 \delta_s / \nu = 2.6 \times 10^4$ and 4.8×10^4 respectively, with $\delta_s \approx 2.8$ in. at both Reynolds numbers. At this station, measurements reported in Part 1 indicated that the boundary layer had the character of an almost self-preserving rough-wall layer. Mean velocity profiles were obtained using a flattened Pitot tube and a Texas Precision Pressure Gage Model 145 which was sensitive to 0.01 mm of water. Surface shear stress was estimated from measurements made with a 0.250 in. o.d., 0.156 in. i.d. Preston tube. A survey of the transverse distribution of wall shear stress at a station on the smooth wall about 2 ft from the end of the roughness showed no significant variation over at least the central 6 in. of the span. For the turbulence measurements a miniature Disa X-probe was used in conjunction with constant-temperature anemometers and the data system described in Luxton, Swenson & Chadwick (1967). The bandwidth of the recorded signals was 2 Hz to 1 kHz.

3. The mean velocity distribution

The co-ordinate system is shown in figure 1. Also shown in this figure are the mean flow streamlines in the vicinity of the rough-to-smooth change in surface. These streamlines were obtained from measurements at the lower of the two

Reynolds numbers investigated. They reveal only small but systematic streamline deflexions associated with the development of the internal boundary layer. It is seen that the streamlines are first displaced at a position which lies almost vertically above the discontinuity in surface, in agreement with the result of Taylor (1962). From this observation, Taylor assumed that the edge of the internal layer was almost perpendicular to the surface. The results in this and the following sections show that no detectable change in the outer flow structure is associated with the small change in the streamlines.

The mean velocity field in the inner region of a smooth-wall turbulent boundary layer is usually described in terms of a logarithmic distribution

$$\frac{U}{U_\tau} = \frac{1}{\kappa} \log \frac{yU_\tau}{\nu} + C, \quad (1)$$

where $U_\tau = \tau_w^{1/2}$ is the kinematic friction velocity based on the local wall shear stress τ_w , κ is the Kármán constant, usually taken as 0.41, and C is a constant which was found by Clauser (1956) to have an average value of 4.9. The Kármán constant and C are assumed to be universal, at least for pressure gradients near zero.

A selection of mean velocity profiles for the two Reynolds numbers investigated are plotted in semi-logarithmic form in figure 2. It is apparent that a linear region exists almost from the first station on the smooth wall and that the extent of this region increases with distance downstream. At the most downstream station which could be studied ($x = 46.1$ in.) the linear region extends over about one decade. If it is assumed† that the value of the Kármán constant κ is indeed constant and equal to 0.41 on the smooth wall downstream from the roughness, then the local wall shear stress distribution may be estimated from the slopes of the linear regions in figure 2. From this and (1) the value of the ‘constant’ C may be obtained as a function of x . The resulting value of C is certainly not constant for this smooth-wall zero-pressure-gradient flow. It decreases rapidly over the first 10 in. from very large values (> 15) and then decreases more slowly to a value of 6.9 at the last measuring station ($x = 46.5$ in.). The large values of C at small values of x , near the change from the rough to the smooth surface, may be subject to quite large errors as the logarithmic region is not well-defined there. However, it is not likely that the errors alter the qualitative trend that C decreases at a rate which is initially very rapid but which becomes more gradual as x increases. The final value is significantly larger than the ‘universal’ value of 4.9 proposed by Clauser (1956), which would suggest that at this station not even the inner region of the boundary layer has completely readjusted to the new surface condition. Examination of the mean velocity profiles obtained by Makita (1968) downstream from a rough-to-smooth surface change in a two-dimensional channel supports the trend for C reported above. Further evidence of this trend may be found in the measurements by Badrinarayanan & Rao (1968) and by Petryk & Brundrett (1967) in the reattached flow field downstream of a single two-dimensional roughness element immersed in a turbulent boundary layer.

† However, see § 4.

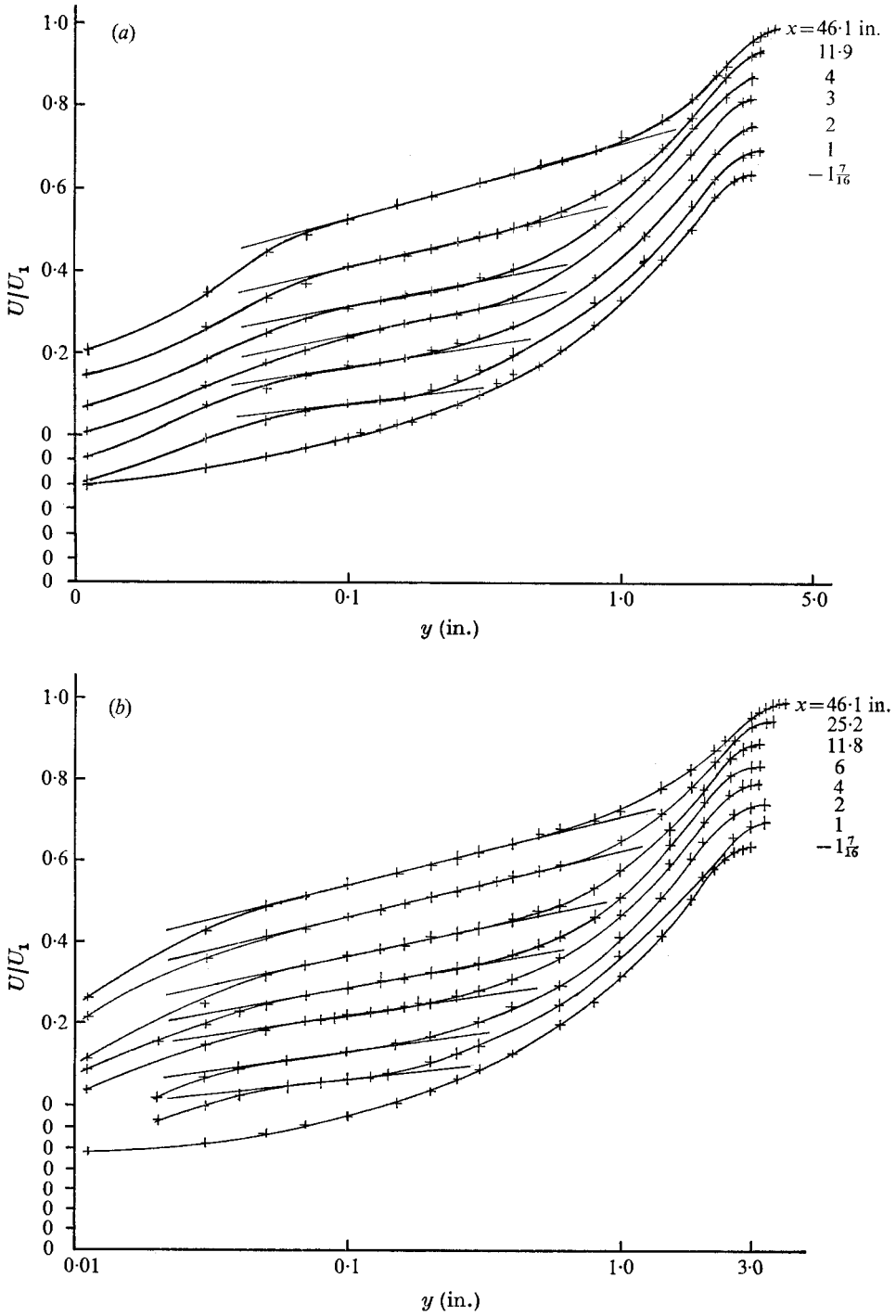


FIGURE 2. Mean velocity profiles on semi-log plots. (a) $U_1 \delta_s / \nu \approx 2.6 \times 10^4$.
 (b) $U_1 \delta_s / \nu \approx 4.8 \times 10^4$. Note shift in origin.

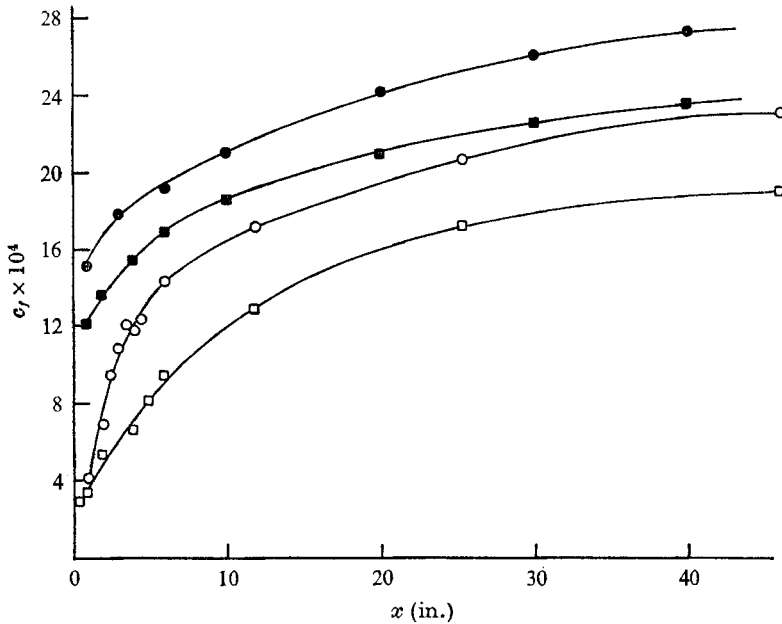


FIGURE 3. Variation of c_f on smooth wall. c_f inferred from semi-log plot of mean velocity profiles (figure 2): ○, $U_1 \delta_s / \nu \simeq 2.6 \times 10^4$; □, 4.8×10^4 . c_f inferred from Preston tube readings: ●, $U_1 \delta_s / \nu \simeq 2.6 \times 10^4$; ■, 4.8×10^4 . At $x = -1\frac{7}{16}$ in. $c_f \simeq 0.0084$ for both values of $U_1 \delta_s / \nu$.

3.1. Estimation of wall shear stress from mean velocity distributions

The distribution of wall shear stress following the roughness change is of obvious practical and theoretical interest. In Part 1 we reported considerable difficulty in determining the effective wall shear stress on the roughness. In the present case we wish to determine the shear stress on the smooth surface downstream from the roughness. While this may appear to be simply a case of applying well-tried smooth-wall boundary-layer techniques it is far from simple to achieve consistency between these techniques.

Wall shear stress values deduced from the slope of the semi-logarithmic plots of mean profiles are compared, in figure 3, with those measured with the Preston tube (for which the Head & Rechenberg (1962) calibration was used). The Preston tube values are consistently higher than those deduced from the slope of the 'log law'. The trend shown by both distributions is, however, the same; the wall shear stress is initially reduced well below the rough-wall value, then increases at a rate which decreases with x . It is still increasing slowly at the last station measured. This trend is in qualitative agreement with the theoretical predictions of Elliott (1958), Panofsky & Townsend (1964) and of Townsend (1965), and with the experimental results of Makita (1968) in a channel and of Taylor (1962) in a boundary layer.†

The Preston tube values shown in figure 3 are probably in error for small values

† The trend in Taylor's (1962) experiments is not as pronounced as that in the present experiments, probably because of the very much smaller magnitude of roughness step and also because Taylor assumed a constant value of $C = 5.5$.

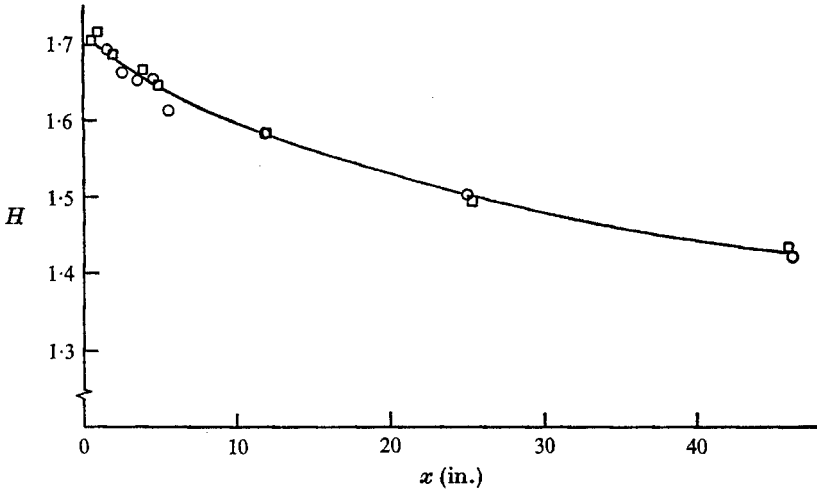


FIGURE 4. Variation of shape parameter with x . ○, $U_1\delta_s/\nu \simeq 2.6 \times 10^4$; □, 4.8×10^4 .

of x (less than about 5 in.) as the Preston tube extended beyond the outer limits of the linear regions shown in figure 2. However, at larger values of x there is less cause to doubt the Preston tube though it must be remembered that the Preston tube calibration relies on the universality of κ and C . The fact that it gives results which lie above those deduced from the 'log law' reflects the non-universality at least of C , and probably also of κ .

The shape parameter H decreases with distance downstream from the step (figure 4) to a value of 1.42 at $x \simeq 46.1$ in. At this station the Reynolds number $R_\theta = U_1\theta/\nu$ (θ being the momentum thickness) is equal to 4250 and 8070 for reference tunnel speeds of 18 and 33 ft/s respectively. The corresponding values of H for a self-preserving boundary layer are 1.36 and 1.33 respectively. Further evidence that the boundary layer is not self-preserving at the last measuring station is obtained by evaluating the defect profile parameter G defined as

$$G = (2/c_f)^{\frac{1}{2}}(1 - 1/H). \quad (2)$$

Using the Preston tube values for c_f , the experimental values for G are 8.04 and 8.56 at $U_1 = 18$ and 33 ft/s respectively. The appropriate value for a self-preserving boundary layer in a zero pressure gradient is about 6.50.

Another commonly used method of evaluating wall shear stress is by application of the momentum integral equation

$$c_f = 2 d\theta/dx, \quad (3)$$

where θ is the momentum thickness and normal stress difference gradients have been ignored. In the present flow this formula suggests a trend which is quite the opposite of that given by the other estimates in figure 4, i.e. c_f seems to decrease monotonically with x . Taylor (1962) found the same trend and pointed out that the estimation of c_f by the momentum integral equation depends on the drawing of a smooth curve through plotted values of θ . It must, therefore,

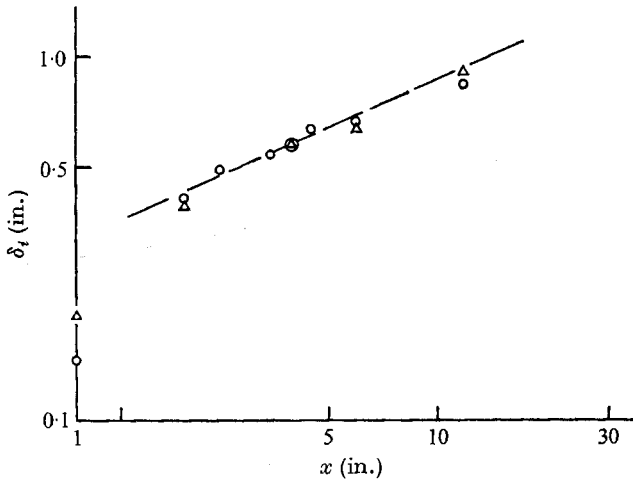


FIGURE 5. Growth of internal layer. \circ , $U_1 \delta_i / \nu \approx 2.6 \times 10^4$; \triangle , 4.8×10^4 ; ---, $\delta_i = 10.3x^{0.43}$.

smooth out any discontinuity in c_f such as that which occurs near the discontinuity in surface roughness. While this observation is correct, it does not fully explain the trend given by (3) as this trend is maintained for some appreciable distance downstream from the discontinuity. Also, near the discontinuity the measurements suggest that $d\theta/dx$ is, within the limited accuracy in this region, very small,† so that if weight is given to these values the resulting distribution of c_f would be unusual, to say the least.

It would seem that none of the standard smooth-wall methods of obtaining skin friction from mean profile measurements is reliable for some distance downstream from the roughness change. Direct measurements of shear stress, using a floating element balance, would be of great value in this region.

4. Growth of internal layer

The edge of the internal layer δ_i is inferred from the approximate merging position of superposed mean velocity profiles obtained at fairly closely spaced stations in the region near the step. The variation of δ_i with x is shown in figure 5 for the two Reynolds numbers investigated. Apart from the estimates of δ_i at the first station, the majority of the points lie reasonably close to the line $\delta_i \propto x^{0.43}$, which represents a significantly slower growth rate than that observed in the case of the smooth-to-rough step (see §6 of Part 1). As was found in Part 1, another convenient method of determining the edge of the internal layer is to plot profiles in the form $U/U_1 \propto y^{1/2}$ (figure 6), although there does not seem to be any sound physical basis for plotting in these co-ordinates.

† Townsend (1956) expects that, in a fully developed boundary layer, the outer flow provides the major contribution to the momentum integral because the mean flow velocity and acceleration are small near the wall. In the region of the discontinuity in surface roughness the outer flow remains unchanged, apart from a small streamline displacement, and hence, as this outer flow provides the major contribution to θ , we would not expect any appreciable rate of change of θ to occur in spite of the large changes which occur in the small region very close to the wall.

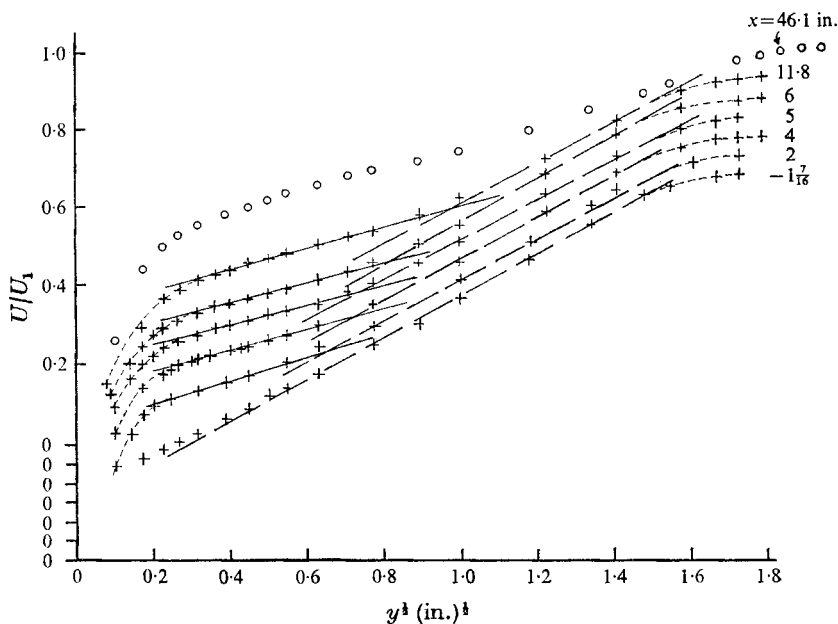


FIGURE 6. Mean velocity profiles plotted as a function of $y^{\frac{1}{2}}$,
 $U_1 \delta_s / \nu \simeq 4.8 \times 10^4$. Note shift in origin.

5. Turbulence intensities: discussion

Figures 7 and 8 show distributions of $\overline{u^2}$ and $\overline{v^2}$, the turbulence intensities in the x and y directions respectively, and of the Reynolds shear stress $-\overline{uv}$ for small values of x at the two Reynolds numbers investigated. The magnitudes of these quantities appear to decrease slightly relative to their respective distributions in the rough-wall boundary layer. This decrease can be seen more clearly on the expanded scale of figure 8(a) than in figure 7(a), but the changes are certainly not as dramatic as those observed in the case of a smooth-to-rough change in surface condition.

Although this decrease is not very pronounced, particularly in the case of $\overline{v^2}$ and $-\overline{uv}$, it is consistent with an increase in $\partial U / \partial x$ (brought about by an increase in the shear stress gradient) and a reduction in $\partial U / \partial y$ (see figure 1). This leads to a decrease in the turbulent energy production $-\overline{uv} \partial U / \partial y$ and hence to a subsequent reduction in the total turbulence energy $\frac{1}{2} \overline{q^2}$ ($\overline{q^2} = \overline{u^2} + \overline{v^2} + \overline{w^2}$). The geometry of the X-probe used did not permit measurements to be made for $y < 0.1$ in., but the trend of the wall shear stress values presented in § 3.1 tends to suggest an increase with x in $-\overline{uv}$ near the wall. This is confirmed to a certain extent by the results of figures 7(b) and 8(b), in which a straight line fitted to the $-\overline{uv}$ measurements nearest to the wall extrapolates to a value at $y = 0$ which is in fair agreement with the surface shear stress value inferred from the slope of the semi-log mean velocity plots. The gradient of $-\overline{uv}$ as indicated by the slope of the straight lines in figures 7(b) and 8(b) clearly decreases with x . At larger values of x , the magnitudes of $\overline{u^2}$, $\overline{v^2}$ and $-\overline{uv}$ shown in figures 9(a).

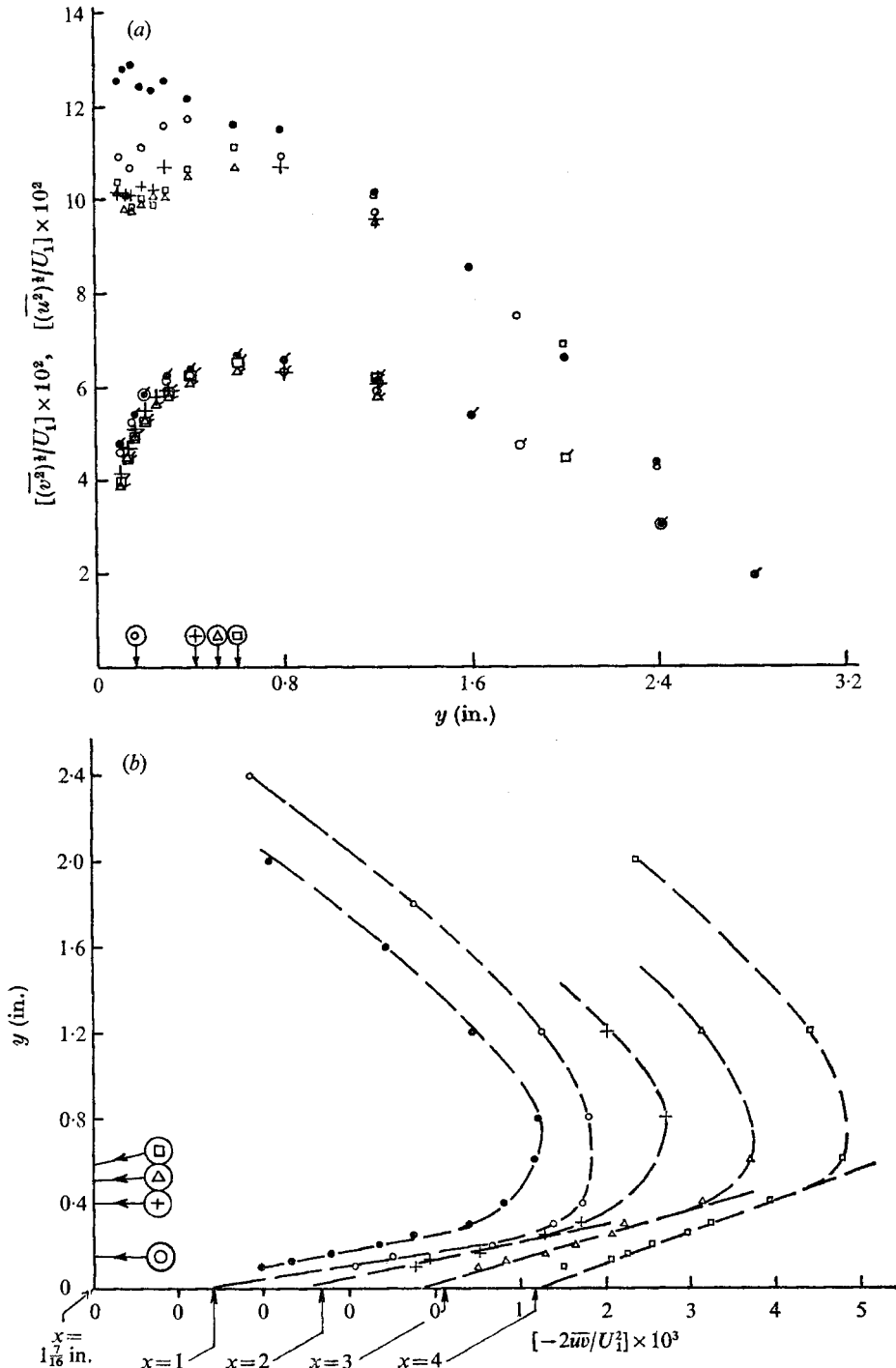


FIGURE 7. Turbulence intensities and shear stress at stations near to the step change in roughness, $U\delta_s/\nu_1 \approx 2.6 \times 10^4$. (a) u and v component intensities. Unflagged symbols refer to $(u^2)^{1/2}/U_1$ and flagged symbols to $(v^2)^{1/2}/U_1$. \bullet , $x = -1\frac{7}{16}$ in.; \circ , 1; +, 2; \triangle , 3; \square , 4. (b) Shear stress $-2\bar{u}'v'/U_1^2$ obtained with an X-wire. Station symbols are as for (a). The arrows indicate values of c , obtained from slope in semi-log plots (figure 2). The arrowed circled symbols in (a) and (b) indicate the approximate positions of the edge of the internal layer at the various stations. Note shift in origin for (b).

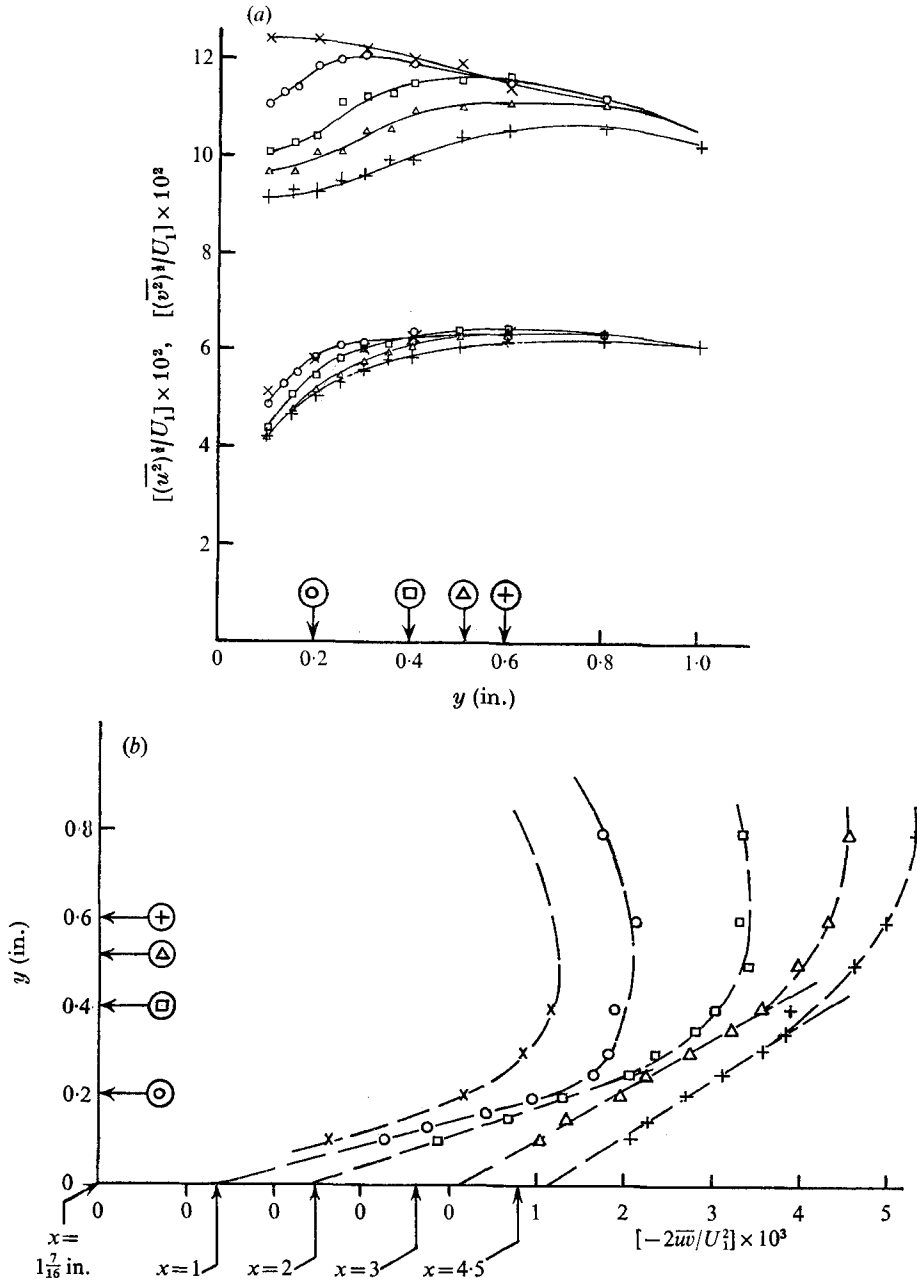


FIGURE 8. Turbulence intensities and shear stress in region near wall, $U_1 \delta_s / \nu \approx 4.8 \times 10^4$. (a) u and v component intensities. Upper distributions are for $(\bar{v}^2)^{1/2}/U_1$. \times , $x = -1\frac{7}{16}$ in.; \circ , 1; \square , 2; Δ , 3; $+$, 4.5. (b) Shear stress $-2\bar{u}\bar{v}/U_1^2$ obtained with an X-wire. Station symbols are as for (a). The arrows indicate values of c_f obtained from slope in semi-log plots (figure 2). The arrowed circled symbols in (a) and (b) indicate the approximate positions of the edge of the internal layer at the various stations. Note the shift in origin for (b).

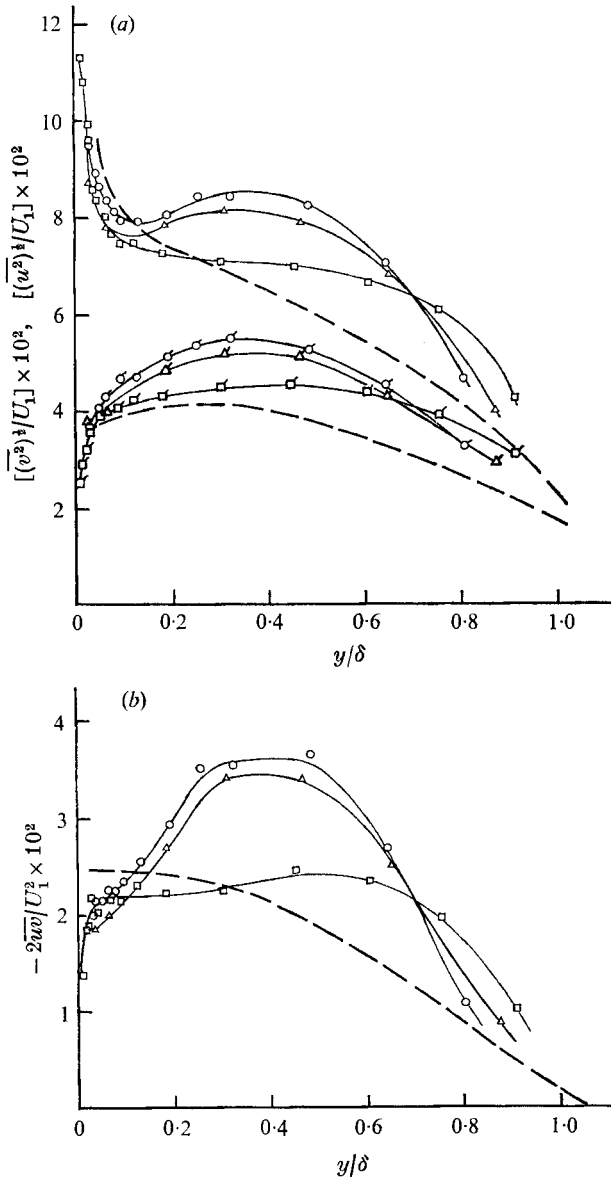


FIGURE 9. Turbulence intensities and shear stress at stations well downstream from the step change in roughness, $U_1 \delta_s/\nu \simeq 2.6 \times 10^4$. (a) u and v component intensities. Unflagged symbols refer to $(u^2)^{1/2}/U_1$ and flagged symbols to $(v^2)^{1/2}/U_1$. (b) Shear stress $-2\overline{uv}/U_1^2$. \circ , $x = 15.9$ in., $\delta = 3.1$ in.; \triangle , $x = 23.3$, $\delta = 3.2$; \square , $x = 45.1$, $\delta = 3.3$; ---, self-preserving distributions on a smooth wall for $U_1 \delta/\nu \simeq 3.1 \times 10^4$.

and 9(b) decrease slowly with x in the outer region of the boundary layer, apparently confirming that the response of the outer flow, which still remembers the large values of u^2 , v^2 and \overline{uv} on the rough wall, is slow.

In figure 9(a), $\overline{u^2}$ rises sharply in the region near the wall, and it is quite likely that this trend first appears in the region $y < 0.1$ in. shown in figures 7(a) and

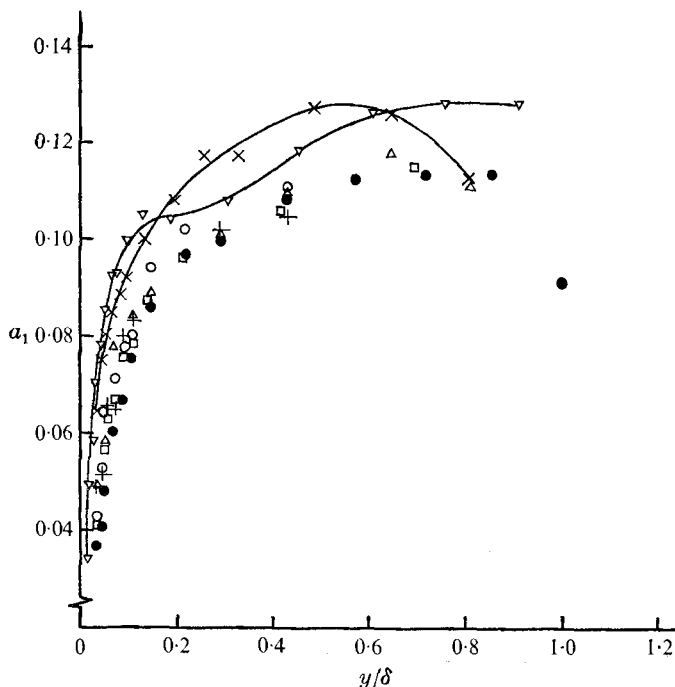


FIGURE 10. Distribution of $a_1 = -\overline{uv}/q^2$ downstream of the step change, $U_1 \delta_s/\nu \simeq 2.6 \times 10^4$.

	●	△	+	○	□	×	▽
x (in.)	$-1\frac{7}{16}$	1	2	3	4	15.9	45.1
δ (in.)	2.8	2.8	2.8	2.8	2.9	3.1	3.3

8(a). At $x = 45.1$ in. the distributions of $\overline{u^2}$, $\overline{v^2}$ and $-\overline{uv}$ in the outer part of the flow are still significantly different from those corresponding to a self-preserving smooth-wall turbulent boundary layer, the distribution of \overline{uv} showing the more marked departure.† In the region close to the wall the distributions of $\overline{u^2}$, $\overline{v^2}$ and $-\overline{uv}$ exhibit shapes which are similar to the self-preserving distributions.‡ In particular, $-\overline{uv}$ in the inner layer is nearly constant and has a value which is in good agreement with the value of $c_f = 0.0023$ inferred from the mean velocity profile at that station (see § 3.1). Makita's (1968) measurements of the turbulence intensities downstream from a rough-to-smooth change in surface condition in a two-dimensional channel also show that $\overline{u^2}$, $\overline{v^2}$ and $-\overline{uv}$ decrease slowly in the streamwise direction in the region away from the wall. Near the surface, however, his measurements indicate a more rapid approach to smooth-wall values than that observed in the present measurements. It is also difficult to reconcile the trend in Makita's values of $-\overline{uv}$ near the wall with the increasing wall shear stress inferred from his mean velocity profiles. The variation of $a_1 = -\overline{uv}/q^2$ is

† The self-preserving distributions shown in figure 9 correspond to $U_1 \delta/\nu = 3.1 \times 10^4$ and to a value of c_f (obtained from a Clauser chart) equal to 0.0025 (see Part 1).

‡ At $x = 45.1$ in., the close proximity to the end of the tunnel enabled measurements to be made as close to the surface as $y = 0.040$ in. It is, however, possible that the proximity to the exit had some influence on the flow.

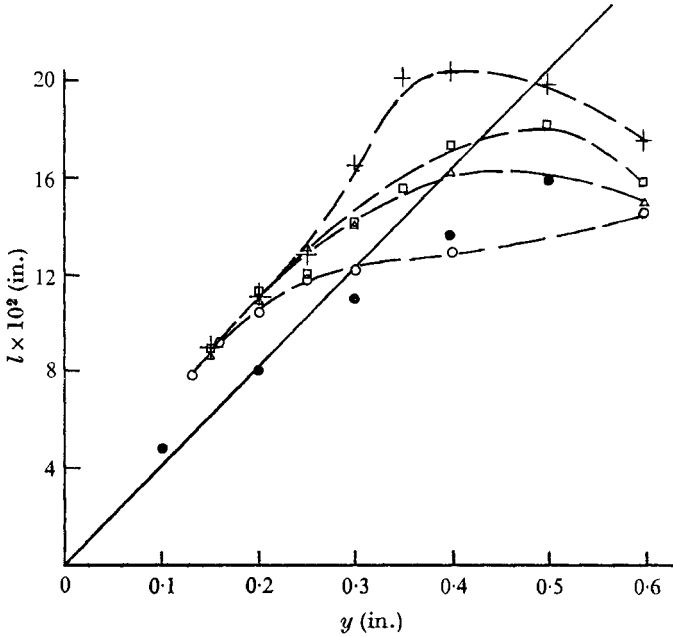


FIGURE 11. Mixing length distributions, $U_1 \delta_s / \nu \simeq 4.8 \times 10^4$. ●, $x = -1\frac{7}{16}$ in.; ○, 1; △, 2; □, 3; +, 4.5; —, $l = 0.41y$.

shown in figure 10.† It is clear that, for small values of x , a_1 is essentially unaffected by the change in boundary condition and retains the same distribution as on the rough wall. This observation is in agreement with the distributions of a_1 reported by Bradshaw & Ferriss (1965) for the initial stage of the response of an equilibrium turbulent boundary layer to the sudden removal of an adverse pressure gradient. As x increases, a_1 slowly increases within the inner layer until at $x = 45.1$ in. it closely resembles the shape obtained in a self-preserving smooth-wall boundary layer (see Part 1). In the outer part of the boundary layer, after an initial rise above its rough-wall self-preserving distribution at $x = 15.9$ in., a_1 gradually decreases with distance downstream suggesting that, in this region of the flow, the decay of $-\overline{wv}$ is slower than that of $\overline{q^2}$.

The mixing length l , defined as $l = \tau^{\frac{1}{2}}(\partial U / \partial y)^{-1}$, rises above its equilibrium rough-wall distribution in the region near the wall for small values of x (figure 11). This trend, which is the opposite of that observed immediately downstream of the smooth-to-rough change discussed in Part 1, seems to throw further doubt on the universality of the log-law constants, particularly κ . The distributions at $x = 2, 3$ and 4.5 in. (figure 11) all exhibit a region which follows the initial increase of l relative to $l = 0.41y$, where l decreases slightly before (presumably) reaching a nearly constant value in the central region of the boundary layer. This slight decrease occurs near the edge of the internal layer and in this region $\partial U / \partial y$, which is reduced inside the internal layer, increases in a relatively short distance and assumes a value corresponding to that over the rough wall. The

† $\overline{q^2}$ is assumed to be equal to $\frac{2}{3}(\overline{u^2} + \overline{v^2})$ as $\overline{w^2}$ was not measured.

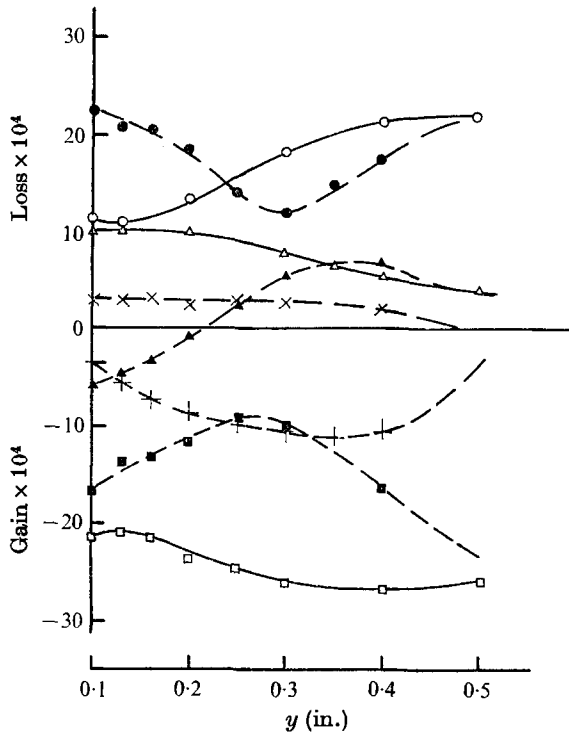


FIGURE 12. Turbulent energy balance across the internal layer at $x = 3$ in., $U_1 \delta/\nu \simeq 2.6 \times 10^4$ and comparison with energy balance on rough wall at $x = -1\frac{7}{8}$ in., $U_1 \delta/\nu \simeq 2.6 \times 10^4$. \square , production by $(\delta/U_1^3) \overline{uv} \partial U/\partial y$; Δ , diffusion by $(\delta/U_1^3) \partial(\frac{1}{2} \overline{q^2} v)/\partial y$ only; \times , production by $(\delta/U_1^3) (\overline{u^2} - \overline{v^2}) \partial U/\partial x$; $+$, advection by $(\delta/U_1^3) (U \partial(\frac{1}{2} \overline{q^2})/\partial x + V \partial(\frac{1}{2} \overline{q^2})/\partial y)$; \circ , dissipation by difference. Open symbols and solid curves are for $x = 3$ in. Closed symbols and broken curves are negligibly small at $x = -1\frac{7}{8}$ in.

determination of $\partial U/\partial y$ is inaccurate in this region and thus it is improper to attach special significance to the described behaviour of l in this region.

6. Turbulent energy balance

The mean flow field and turbulence data presented in the previous sections can be further discussed in terms of a turbulent energy balance. The various terms in the turbulent energy equation

$$U \frac{\partial}{\partial x} (\frac{1}{2} \overline{q^2}) + V \frac{\partial}{\partial y} (\frac{1}{2} \overline{q^2}) + \overline{uv} \frac{\partial U}{\partial y} + \frac{\partial}{\partial y} (\frac{1}{2} \overline{q^2} v + \overline{pv}) + \epsilon = 0, \tag{4}$$

made dimensionless with U_1 and δ , are plotted in figure 12 for the region of the flow corresponding approximately to the internal layer at $x = 3$ in. Also shown in figure 12 are the corresponding distributions on the rough wall at $x = -1\frac{7}{8}$ in. The turbulent intensity $\overline{q^2}$ is again assumed to be given by $\overline{q^2} = \frac{3}{2}(\overline{u^2} + \overline{v^2})$ and the pressure diffusion term \overline{pv} is boldly neglected. The dissipation ϵ is obtained by difference.

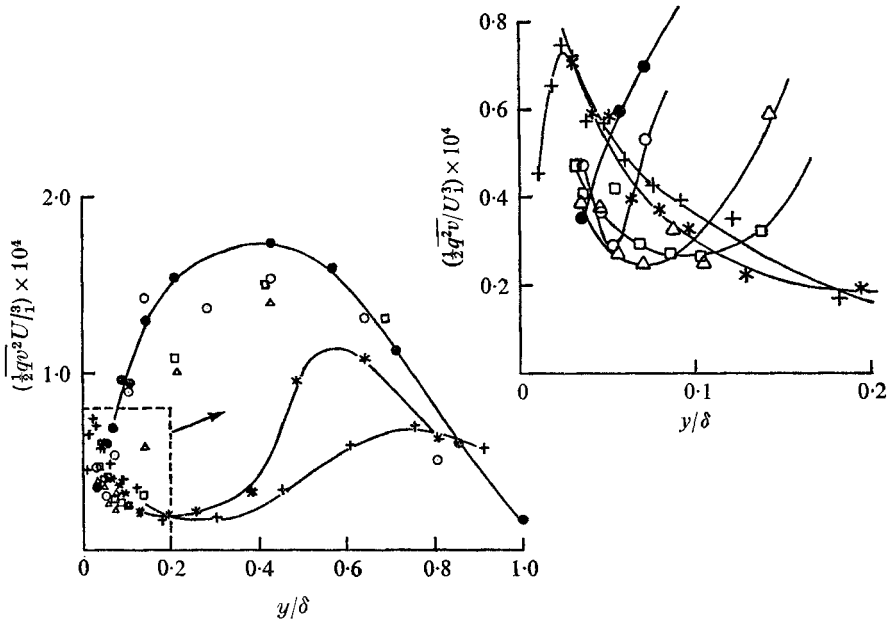


FIGURE 13. Distributions of diffusion energy flux, $U_1 \delta_s / \nu \simeq 2.6 \times 10^4$. Points for $y/\delta < 0.2$ are replotted in top right-hand figure. ●, $x = -1\frac{7}{16}$ in.; ○, 1; △, 3; □, 4; *, 15.9; +, 45.1.

The production of turbulent energy by $-\overline{uv}(\partial U/\partial y)$ is, as expected, decreased relative to its distribution on the rough wall since $-\overline{uv}$ and $\partial U/\partial y$ are both reduced as seen previously. Although the shear stress $-\overline{uv}$ is far from constant in the region near the surface change (see figures 7(b) and 8) the zero-pressure-gradient condition requires $\partial \tau/\partial y = 0$ at the wall, where $\tau = -\overline{uv} + \nu(\partial U/\partial y)$, and hence the maximum value of $-\overline{uv}(\partial U/\partial y)$ near the wall may be shown to be $\tau_w^2/4\nu$. When the wall shear stress value inferred from the slope of the semi-log mean velocity plot at $x = 3$ in. is used, it is found that $\delta/U_1^3 [-\overline{uv}(\partial U/\partial y)]_{\max}$ is approximately 18×10^{-4} , which is smaller than the value of the 'secondary' peak (about 27×10^{-4} at $y \simeq 0.4$ in.) on the rough wall.† It seems likely that, for small values of x at least, the flow near the wall is affected by the high values of $-\overline{uv}(\partial U/\partial y)$, and presumably of q^2 , which occur away from the wall. As x increases, however, the wall shear stress rises while the value of the secondary peak decreases. It then appears likely that the wall shear stress will quickly become of primary importance in determining the flow near the wall. The production of turbulent energy by the interaction of the normal stresses with the streamwise mean velocity gradient, $(\overline{u^2} - \overline{v^2})\partial U/\partial x$, is small compared with $-\overline{uv}(\partial U/\partial y)$ but is significant when compared with the diffusion. As the edge of the internal layer is approached (the mean velocity profiles indicate that at $x = 3$ in. this edge lies at $y \simeq 0.50$ in.) the distributions of $-\overline{uv}(\partial U/\partial y)$ and of

† The maximum value of $-\overline{uv}(\partial U/\partial y)$ on the rough wall occurs very near the crest of the roughness and is appreciably larger than the observed 'secondary' peak value which occurs some distance from the surface (see Part 1).

the other terms of the energy balance tend to become similar to the corresponding distributions over the rough wall (Antonia & Luxton 1971*a*).

The shape of the diffusion curve at $x = 3$ in. is significantly different from that on the rough wall and indicates a small gain of energy in the region close to the wall. This may be due in part to the diffusion of energy down the gradient of \bar{q}^2 ($\partial\bar{q}^2/\partial y$ is positive inside the internal layer for $y > 0.15$ in. approximately) from the region of large $-\bar{w}\bar{v}(\partial U/\partial y)$ and \bar{q}^2 mentioned above. In the region $y < 0.1$ in., $\partial\bar{q}^2/\partial y$ is probably negative as \bar{q}^2 has a tendency to rise in the immediate vicinity of the wall and it is likely that there energy is diffused out from the wall down the gradient of \bar{q}^2 . Near $y = 0$, the shapes of the distributions of $\frac{1}{2}\bar{q}^2\bar{v}$ in figure 13 suggest a loss of energy.† Figure 13 also shows that the region near the wall which is associated with a gain of energy tends to increase with increasing x , lending support to the idea that the wall becomes increasingly important with distance downstream. The distribution of $\bar{q}^2\bar{v}$ at $x = 45.1$ in. is similar to that for a self-preserving smooth-wall turbulent boundary layer (see Part 1) in the region $y/\delta < 0.4$. Near the edge of the boundary layer the slope of $\frac{1}{2}\bar{q}^2\bar{v}$ is reduced relative to that on the rough wall.

The most striking feature of the energy balance results is the large gain of energy by advection, which is comparable in magnitude with the production term $-\bar{w}\bar{v}(\partial U/\partial y)$.‡ The term $U(\partial\bar{q}^2/\partial x)$ provides the major contribution to the advection as both U and $\partial\bar{q}^2/\partial x$ are increased near the step. The contribution from $V(\partial\bar{q}^2/\partial y)$, although small, is of the same sign as $U(\partial\bar{q}^2/\partial x)$ as V is negative and $\partial\bar{q}^2/\partial y$ remains essentially positive in the region considered in figure 12. The relatively large value of the advection term clearly shows that even the inner part of the internal layer is almost certainly not in local equilibrium (Townsend 1961).

The dissipation has the same shape as the production (by $-\bar{w}\bar{v}(\partial U/\partial y)$) and is equal to it for $y > 0.3$ in. The dissipation tends to be slightly larger than the production in the region $y < 0.3$ in., but the assumption that they are nearly the same is reasonable within the accuracy of the measurements. The dissipation length scale L_ϵ is therefore approximately equal to the mixing length l which, as shown earlier, increases at a faster rate than that given by $l = \kappa y$. It should be noted that the increase in l above $0.41y$ is also supported by an increase in the integral length scale (obtained via Taylor's hypothesis from the area under the autocorrelation curve for the longitudinal velocity fluctuations) in the region near the step change in surface condition. Following a streamline, this increase occurs very nearly at a position corresponding to the edge of the internal layer. Further support for the increase in l may be found in the results of Busch & Panofsky (1968) for flow downstream from a rough-to-smooth step in the atmospheric boundary layer. Bradshaw (1969) explains this increase in l qualitatively

† It should be noted that the accuracy of the measurements of $\frac{1}{2}\bar{q}^2\bar{v}$ near $y = 0$ is poorer than that of those further away from the surface owing to the combined effects of non-linearities in the anemometers, and phase shifting in the data system. For further detail, see Part 1.

‡ Note that the advection in the corresponding region of the rough wall is negligibly small.

by considering the equation for the rate of change of shear stress along a mean streamline in the vicinity of the step change. His analysis assumes, however, that the length scale for the stress containing part of the turbulence is given by κy and that the turbulent diffusion is small. This latter assumption does not appear to hold in the inner region of the rough-wall layer (see Antonia & Luxton 1971*a*).

7. Discussion

The experimental results presented in the preceding sections appear to indicate that the response of a zero-pressure-gradient turbulent boundary layer to a rough-to-smooth change in surface is slower than the smooth-to-rough response which was studied in Part 1.

Townsend (1965) has suggested that the time required for a substantial adjustment of the turbulent energy or Reynolds shear stress downstream from a step change in surface roughness is of the order of the turbulent energy divided by the production of turbulent energy. The minimum distance before a substantial change can be observed in the Reynolds shear stress or the turbulent energy of a fluid parcel entering a region of changed rate of strain may then be written as the product of this time and the local velocity U , i.e.

$$x = \frac{-\bar{q}^2}{2\bar{u}\bar{v}} y \log \frac{y}{z_0}, \quad (5)$$

where z_0 is the characteristic roughness length scale for the rough surface.

Although (5) may be regarded as a simple implicit relation for the growth of the internal layer, the basic underlying assumption in its formulation is that the unperturbed flow is responsible for the rate of propagation of the disturbance. Neither the magnitude nor the nature of the roughness is included in the argument. Further, it is clear that the new rate of strain is not instantaneously applied throughout the inner layer and consequently (5) can only reasonably predict the adjustment distance over a very limited range of y . It is also noted that (5) predicts a faster response for the rough-to-smooth step, as the mean velocity near the rough wall is smaller than that near a smooth wall at an equivalent Reynolds number. The observed reduction in α_1 near a rough wall is not sufficiently large to affect this result, which is clearly at variance with experimental evidence.

Bradshaw (1967) has indicated that an estimate of the strength of the perturbation may be the ratio of the integrated advection to the integrated production at any station downstream from the perturbation. This ratio is found to be significantly larger in the case of a turbulent boundary layer which is subjected to a sudden removal of its adverse pressure gradient (Bradshaw & Ferriss 1965) than in the case of a constant-pressure boundary layer which passes into a region of fairly strong adverse pressure gradient (Bradshaw 1967). The response of the boundary layer to the sudden removal of the pressure gradient is correspondingly slower. Downstream from a step change in surface roughness the advection in the region outside the internal layer remains the same as in the

unperturbed layer upstream and is therefore negligible compared with the production except, of course, near the edge of the boundary layer. In the region near the wall, however, the advection represents a significantly larger proportion of the production for the rough-to-smooth than for the smooth-to-rough step. It must be pointed out here that at least the initial stage of the response of a turbulent boundary layer to the sudden application or removal of the pressure gradient will be different from that to a step change in roughness, mainly because of the manner in which the perturbation is applied. The step change in the pressure gradient is applied throughout the whole flow but the Reynolds shear stress in the outer layer readjusts slowly since, as Bradshaw & Ferriss (1965) have pointed out, the step change in dP/dx results in a quadratic change (with respect to time or distance) in $-\bar{uv}$ or q^2 . In the region near the wall, the rates of energy production and dissipation remain large compared with the rate of energy gain by advection and the inner layer is thus closely in equilibrium, unlike the inner part of the internal layer downstream from a roughness step.

It is of interest to note that the boundary-layer flow downstream from a rough-to-smooth step exhibits the same trend for the variation of the integral parameters such as c_f or H as that downstream from the sudden removal of an adverse pressure gradient (Bradshaw & Ferriss 1965), downstream of re-attachment from a single two-dimensional fence (Mueller & Robertson 1962), or downstream from a sudden discontinuation in injection at the surface (Levitch†). This common behaviour must apparently be attributed to the decreased rate of strain, but it is also seen that the distributions of the Reynolds shear stress in the undisturbed boundary layer immediately upstream, and also in the perturbed flow downstream, from the application of the perturbation are somewhat similar for all of the cases mentioned above. However, apart from this evidence, the importance of the flow structure upstream of the surface change in dictating the response must as yet be regarded as unproven.

From the experimental results presented in this paper and in Part 1, it is difficult to say clearly whether the turbulence structure of the flow upstream of the surface change is of primary importance in dictating the growth of the new layer or whether the magnitude (and nature) of the roughness step is of equal if not greater importance. One of the main features of the early stage of the response to the smooth-to-rough step is the diffusion of turbulent energy away from the rough surface. This tends to suggest that the magnitude of the step may be the controlling parameter for determining the rate of spread of the perturbation. To check this suggestion, it is recommended that further experimental investigations be carried out for the smooth-to-rough step for various magnitudes of the step.

The rough-to-smooth response studied here is characterized mainly by the advection of turbulent energy from the upstream rough-wall boundary layer. Although it is likely that there is a significant diffusion of energy away from the smooth wall, it also appears that the central region of the perturbed layer receives energy (by diffusion) from the outer part of the internal layer, emphasizing the dominant role played by the external unperturbed flow. To test the importance

† Some of the results of Levitch are reported in Tani (1968).

of the external flow it is recommended that further experimental studies be made of the response to a rough-to-rough step, with the surface downstream from the step being different in magnitude or type from that upstream, and of the response to a smooth-to-rough step in an adverse pressure gradient.

8. Conclusions

The present experimental results indicate that a nearly self-preserving turbulent boundary layer in a zero pressure gradient adjusts rather slowly following a rough-to-smooth change in the surface condition. Contrary to the usual assumption, the slow adjustment is a feature of both the inner and outer layers.

Although a logarithmic mean velocity distribution is observed in the region near the wall almost immediately downstream of the rough-smooth junction, the constant C (see equation (1)) is found to be appreciably higher than the 'universal' smooth-wall value. The mixing length distributions in this region suggest that κ is also larger than the usual value of 0.41. Because of this non-universality of κ and C the determination of the skin-friction coefficient from a Clauser chart or by a Preston tube is somewhat uncertain. Direct measurements of the wall shear stress using a floating-element technique would be of great value, particularly in the region near the step.

The mean velocity and the turbulence intensity distributions at the last available station had not reached self-preservation. In particular, the Reynolds shear stress increases throughout the central region of the boundary layer instead of monotonically decreasing as is expected for a given self-preserving zero-pressure-gradient layer. A possible reason for the long 'memory' in a rough-wall boundary layer may be that a large proportion of the turbulent energy resides in the larger scale turbulence in the outer part of the layer rather than in the smaller scale turbulence closer to the wall.

An analysis of the turbulent energy equation for the internal layer in the region near the step shows that the production and the dissipation terms are almost equal but the contribution from the advection is comparable with these terms. This result, together with the observed increase in the mixing length near the wall, emphasizes the non-equilibrium behaviour of the wall region of the internal layer. All those theoretical models for the response of the turbulent boundary layer to a step change in surface roughness which effectively assume that equilibrium conditions exist downstream from the step are unlikely to predict the flow changes in this region accurately. The diffusion results presented demonstrate convincingly the differences in the internal-layer structure in the rough-to-smooth and the smooth-to-rough cases. In the latter case, the velocity of propagation of the internal layer depends mainly on the turbulence intensity within this layer. In the rough-to-smooth case, the highly turbulent outer layer tries to compensate for the fall in energy production near the wall, with the result that the rate of growth of the internal layer depends both on the outer layer and on conditions within the internal layer. Although the initial stage of the rough-to-smooth response appears to be dominated by the advection of

energy from the upstream rough-wall boundary layer, there is little doubt that, as the distance downstream from the step increases, the wall becomes of increasing importance in controlling the turbulence structure in the inner layer.

The work described in this paper represents part of a programme of research supported by grants from the Australian Research Grants Committee, the Australian Institute of Nuclear Science and Engineering, and the Commonwealth Scientific and Industrial Research Organization.

REFERENCES

- ANTONIA, R. A. & LUXTON, R. E. 1971*a* *Phys. Fluids*, **14**, 1027.
ANTONIA, R. A. & LUXTON, R. E. 1971*b* *J. Fluid Mech.* **48**, 721.
BADRINARAYANAN, M. A. & RAO, K. N. 1968 *Aero. Soc. of India, Joint Technical Sessions, Bangalore*.
BRADLEY, E. F. 1965 Ph.D. thesis, Australian National University.
BRADSHAW, P. 1967 *N.P.L. Aero Rep.* no. 1219.
BRADSHAW, P. 1969 *J. Atmos. Sci.* **26**, 1353.
BRADSHAW, P. & FERRISS, D. H. 1965 *N.P.L. Aero Res.* no. 1145.
BUSCH, N. E. & PANOFSKY, H. A. 1968 *Quart. J. Roy. Met. Soc.* **94**, 132.
CLAUSER, F. H. 1956 *Advances in Appl. Mech.* **4**, 1.
ELLIOTT, W. P. 1958 *Trans. Am. Geophys. Union*, **39**, 1048.
HEAD, M. R. & RECHENBERG, I. 1962 *J. Fluid Mech.* **14**, 1.
JACOBS, W. 1939 *Z. angew. Math. Mech.* **19**, 87. (Trans. 1940 *N.A.C.A. Tech. Memo.* no. 951.)
LUXTON, R. E., SWENSON, G. G. & CHADWICK, B. S. 1967 *The Collection and Processing of Field Data* (ed. E. F. Bradley & O. T. Denmead), p. 497. Interscience.
MAKITA, H. 1968 M. Eng. thesis, University of Tokyo.
MUELLER, R. J. & ROBERTSON, J. M. 1962 *Proc. 1st South. Conf. Theor. Appl. Mech., Gatlinburg, Tenn.* p. 326.
PANOFSKY, H. A. & TOWNSEND, A. A. 1964 *Quart. J. Roy. Met. Soc.* **90**, 147.
PETRYK, S. & BRUNDRETT, E. 1967 *Dept. of Mech. Eng, University of Waterloo Research Rep.* no. 2.
TANI, I. 1968 *Proc. Computation of Turbulent Boundary Layers, AFOSR-IFP--Stanford University*.
TAYLOR, R. J. 1962 *J. Fluid Mech.* **13**, 529.
TOWNSEND, A. A. 1956 *The Structure of Turbulent Shear Flow*. Cambridge University Press.
TOWNSEND, A. A. 1961 *J. Fluid Mech.* **11**, 97.
TOWNSEND, A. A. 1965 *J. Fluid Mech.* **22**, 773.